PHYSICAL REVIEW A VOLUME 46, NUMBER 11 1 DECEMBER 1992

Planar ion microtraps

R. G. Brewer, R. G. DeVoe, and R. Kallenbach
IBM Research Division, Almaden Research Center, San Jose, California 95120-6099
(Received 14 May 1992)

Planar quadrupole ion traps have been analyzed through numerical and analytic solutions of Laplace's equation. These involve either one or more conducting rings or their analogs, a hole in one or more conducting sheets. The leading terms in the potential are harmonic, corresponding to the Paul trap, but with coefficients that reduce their efficiency and for some traps, the anharmonic terms can be suppressed to eighth order. Stable ion trapping is predicted for all electrode configurations possessing radial and axial symmetry. A three-hole microtrap with an inner hole radius of 80 μm trapped from one to many (dense clouds) laser-cooled Ba^+ ions where the two-ion distance is compressed to 1 μm, allowing new experiments in quantum optics. Also, arrays of traps for optical clocks are contemplated using photolithographic fabrication.

PACS numbers: 32.80.Pj, 42.50. Vk

Several fundamental atomic-physics experiments have been performed recently [1, 2] using a Paul trap [3]. One or more ions can be stored for days under conditions of ultrahigh vacuum and millikelvin or lower temperatures, making them almost motionless and free of perturbations. Hence, these systems are ideal candidates for atomic clocks or other precision spectroscopic measurements. In a Paul trap of radius $\bar{r}$, the ions are stored by virtue of a cylindrically symmetric electric quadrupole potential

$$V = (V_{\rm dc} + V_{\rm ac}\cos\Omega t)[z^2 - \rho^2/2]/\bar{r}^2 \qquad (1)$$

that oscillates at an rf frequency Ω across hyperboloidal electrodes, two end caps and a ring. A variation of the Paul trap has been realized also in a one-ring trap [4], a linear trap [5], and one with cones of revolution [6].

Current Paul traps, however, keep the ions sufficiently far apart that interesting phenomena such as superradiance cannot be observed. In the case of two ions, for example, solutions to the modified Mathieu equations of motion give an ion-ion distance $R = 2[e^2/(m\omega_r^2)]^{1/3}$ where e and m are the charge and mass of one ion, the secular frequencies $\omega_{z,r} = \beta_{z,r}\Omega/2$, the Floquet exponents $\beta_{z,r} \cong q_{z,r}/\sqrt{2}$, and the dimensionless Mathieu parameter $q \equiv q_z = 2q_r = 4eV_{\rm ac}/(m\Omega^2\bar{r}^2)$. Since $R \propto \Omega^{-2/3}$ when q is fixed, increasing the rf frequency Ω reduces R. This in turn requires that the trap dimension $\bar{r}$ decrease so that $(\Omega\bar{r})^2$ and thus q_z remain essentially constant.

In this article, we consider other variations of a Paul trap where the electrodes are of a simple planar geometry that permits precise photolithographic fabrication of a microtrap on a micrometer scale [7]. Clearly, the difficulty of the precision machining of hyperboloidal surfaces in small dimensions argues against a conventional Paul trap. The simplest example is a one-hole trap, Fig. 1(a), a metallic sheet with one circular hole dividing two uniform electric fields. It is the analog of a one-ring trap, Fig. 1(b). A larger trapping volume and a deeper potential well occur in the three-hole trap, Fig. 1(c), and its analog, the three-ring configuration, Fig. 1(d). These traps approximate the Paul trap near the trap origin where they are harmonic; away from the origin, the first three become increasingly anharmonic, whereas the three-ring trap is easily compensated to eighth order. All of these traps are optically accessible through a large solid angle that improves the laser cooling of ions and detection of ion-scattered laser light. Moreover, these traps can be fabricated lithographically in micrometer dimensions, either individually or in an array, the latter being particularly appealing in the case of an atomic clock where the signal strength improves the accuracy over a one-ion clock [8]. We thus foresee the possibility of ion-trap and integrated-circuit technology merging with a single chip containing the trap, diode lasers, and associated electronics.

One-hole trap. Assume an extended thin metal sheet with a hole of radius $\rho = a$ and bounded by a uniform field E_0 for $z \geq 0$ and E_1 for $z \leq 0$ with $E \equiv E_0 = -E_1$. This configuration is a quadrupole potential where the two outer electrodes lie at $z = \pm\infty$ with an ∞ potential. An exact expression for the potential in terms of oblate spherical coordinates [9] is

$$\Phi(\varepsilon,\zeta) = \frac{2}{\pi}aE\varepsilon(\zeta\tan^{-1}\zeta + 1), \qquad (2)$$

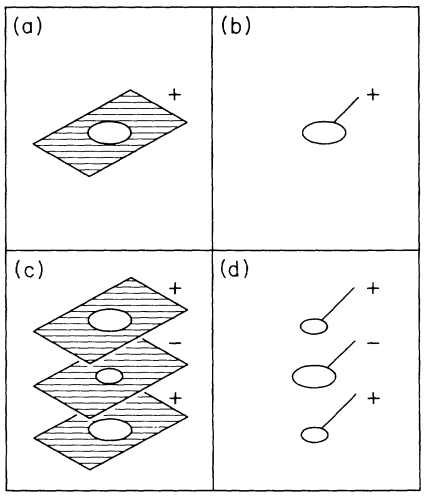

FIG. 1. Schematic of planar Paul traps made from conducting rings or holes in conducting sheets. (a) One-hole trap. (b) One-ring trap. (c) Three-hole trap. (d) Three-ring trap.

where $0 < \varepsilon < 1$ and $-\infty < \zeta < \infty$. In terms of cylindrical coordinates $(\rho/a)^2 = (1-\varepsilon^2)(1+\zeta^2)$ and $z = a\zeta\varepsilon$ or inversely, $\zeta^2 = \{(r/a)^2 - 1 + \sqrt{[1-(r/a)^2]^2 + 4(z/a)^2}\}/2$ where $r^2 = \rho^2 + z^2$. Alternatively, the potential can be expressed as an integral [10] or in the trapping region $r < a$ as a Legendre series in spherical coordinates

$$\Phi(r,\theta) = \frac{2}{\pi} Ea \left[\sum_{n=0}^{\infty} \frac{(-1)^{n+1}}{2n-1} \left(\frac{r}{a}\right)^{2n} P_{2n}(\cos\theta) \right], \tag{3}$$

where $\cos\theta = z/r$. From Eq. (2) we see that $\lim_{\rho\to 0} \Phi(\rho,z) = \frac{2}{\pi} Ea(1 - \frac{z}{a}\tan^{-1}\frac{a}{z}) + Ez$ and $\lim_{z\to 0} \Phi(\rho,z) = \frac{2}{\pi} Ea\sqrt{1-(\rho/a)^2}$, so that the potential at the origin is $\Phi(0,0) = \frac{2}{\pi} Ea$ and at the edge of the hole is $\Phi(a,0) = 0$. Moreover, by expanding either Eq. (2) or (3) and taking the gradient of $-e\Phi(\rho,z)$, we obtain the leading terms in the axial and radial components of the reduced force on an ion in the presence of a field $E(t) = E_0 \cos(\Omega t)$,

$$\frac{\ddot{z}}{a} = 2q\cos(2\tau)\left[-\frac{z}{a} + \frac{2}{3}\left(\frac{z}{a}\right)^3 - \frac{\rho^2 z}{a^3} + \cdots\right], \tag{4}$$

$$\frac{\ddot{\rho}}{a} = q\cos(2\tau)\left[\frac{\rho}{a} + \frac{1}{2}\left(\frac{\rho}{a}\right)^3 - 2\frac{\rho z^2}{a^3} + \cdots\right]. \tag{5}$$

Here, time $\tau = \Omega t/2$ and $q = 8eE_0 a/(\pi m\Omega^2 a^2)$ are dimensionless. The linear terms of Eqs. (4) and (5) correspond to the Paul trap, Eq. (1), and result in trapping but with a slightly reduced force due to the efficiency factor $\epsilon \equiv q/q_{\text{Paul}} = 2/\pi$ appearing in the q term. The remaining anharmonic terms become important as an ion moves away from the trap origin.

Three-hole trap. This trap consists of three thin parallel metal sheets with three concentric holes as in Fig. 1(c). The inner hole is of radius a, the outer two holes are of radius $\bar{a}$, and the spacing between adjacent sheets is b. Application of a potential between the inner and the two outer sheets produces a quadrupole. Clearly, as $b \to \pm\infty$, the three-hole trap reduces to the one-hole trap. The considerable advantage of the three-hole trap over the one-hole trap is that it requires a lower applied voltage for the same trap potential. Since analytic solutions are not known for this case [see Eq. (10) for a partial solution], numerical solutions of Laplace's equation were obtained for the experimental configuration $(a,\bar{a},b) = (50,75,50)$ μm for metal sheets of 225-μm radius and 25-μm thickness. The axial field for an applied voltage of 1 V is shown in Fig. 2, where other traps are compared.

One-ring trap. The potential of an infinitely thin ring of radius a and with a charge Q is given by the Legendre series $\Phi_<(r,\theta) = \frac{Q}{a}\sum_l (\frac{r}{a})^l P_l(0) P_l(\cos\theta)$ for $r < a$ and by $\Phi_>(r,\theta) = \frac{Q}{r}\sum_l (\frac{a}{r})^l P_l(0) P_l(\cos\theta)$ for $r > a$ where $\cos\theta = z/r$ and $r^2 = \rho^2 + z^2$ [10]. This too is a quadrupole potential with outer electrodes at $z = \pm\infty$ but at zero potential. First, we relate the charge Q to an applied potential ϕ through the ring capacity $C = Q/\phi$. Here, $C = \frac{\pi a}{\ln(8a/d)}$ [11], which is nonzero when the cross-sectional ring radius $d > 0$. Considering only the trapping region, $r < a$, an oscillating potential $\phi_a \cos(2\tau)$ generates the reduced force components

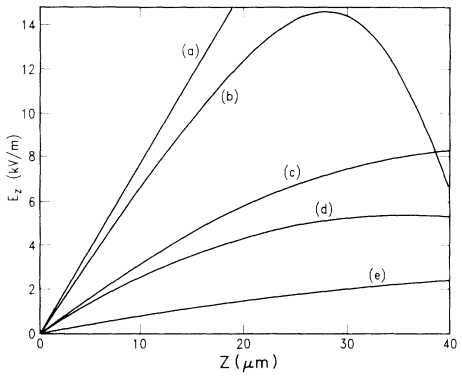

FIG. 2. Electric field E_z vs z at $\rho = 0$ numerically derived from Laplace's equation for various all metal Paul microtraps. The inner and outer electrodes have a peak potential of 1 and 0 V, respectively. (a) Paul trap with radius $\bar{r} = 50$ μm and efficiency $\epsilon = 1$. (b) Compensated three-ring trap with $(a,\bar{a},b,d) = (50, 19.0819, 41.6712, 5)$ μm and $\epsilon = 0.55$. (c) Three-hole trap with $(a,\bar{a},b,\text{thickness},\text{width}) = (50,75,50,25,450)$ μm and $\epsilon = 0.39$. (d) One-ring trap with $(a,d) = (50,5)$ μm and $\epsilon = 0.36$. (e) One-hole trap with $(a,\bar{a},b,\text{thickness},\text{width}) = (50,0,300,0,1600)$ μm and $\epsilon = 0.1$.

$$\frac{\ddot{z}}{a} = 2q\cos(2\tau)\left[\frac{z}{a} - \frac{3}{2}\left(\frac{z}{a}\right)^3 + \frac{9}{4}\frac{z\rho^2}{a^3} - \cdots\right], \tag{6}$$

$$\frac{\ddot{\rho}}{a} = q\cos(2\tau)\left[-\frac{\rho}{a} - \frac{9}{8}\left(\frac{\rho}{a}\right)^3 + \frac{9}{2}\frac{\rho z^2}{a^3} - \cdots\right], \tag{7}$$

where $q = (C/2a)(4e\phi_a)/(m\Omega^2 a^2)$. The linear trapping terms in Eqs. (6) and (7) again emerge but with an efficiency factor $\epsilon = C/2a = \frac{\pi}{2\ln(8a/d)}$ appearing in the q term. Comparing these equations with Eqs. (4) and (5), we see that a one-ring trap is more anharmonic than a one-hole trap. In addition, the Paul-Straubel trap of Ref. [4] with dimensions (a, width, thickness)=(50,200,50) μm is neither a thin one-ring trap nor a thin one-hole trap, and requires numerical solutions of Laplace's equation, the efficiency being $\epsilon = 0.13$.

Three-ring trap. Consider Fig. 1(d) where a quadrupole potential results from an inner ring of radius a and charge Q and two outer rings each of radius $\bar{a}$ and charge $-Q/2$, the spacing between adjacent rings being b. The combined potentials at a point in space (r,θ) are given by the Legendre series $\Phi_<(r,\theta) = \frac{Q}{r_0}\sum_{n=0}^{\infty} a_{2n}(\frac{r}{r_0})^{2n} P_{2n}(\cos\theta)$ for $r < r_0$ and by $\Phi_>(r,\theta) = \Phi_<(r \leftrightarrow r_0)$ for $r > r_0$, where $r_0^2 = \bar{a}^2 + b^2$ and the odd order terms vanish. The coefficients $a_{2n} = P_{2n}(b/r_0) - \alpha^{2n+1} P_{2n}(0)$ with $\alpha = r_0/a$. Proceeding as in the one-ring trap, the leading terms in the reduced force equations are

$$\frac{\ddot{z}}{r_0} = 2q\cos(2\tau)\left[-\frac{z}{r_0} + \frac{a_4}{a_2}\left(-\frac{2z^3}{r_0^3} + \frac{3z\rho^2}{r_0^3}\right) + \cdots\right], \tag{8}$$

$$\frac{\ddot{\rho}}{r_0} = q\cos(2\tau)\left[\frac{\rho}{r_0} + 3\frac{a_4}{a_2}\left(\frac{\rho^3}{2r_0^3} - \frac{3\rho z^2}{r_0^3}\right) + \cdots\right]. \tag{9}$$

Here, $q = (Ca_2/r_0)(4e\phi/m\Omega^2 r_0^2)$, and the linear terms result in trapping with an efficiency $\epsilon = Ca_2/r_0$, where C is the three-ring capacity and $\phi\cos(2\tau)$ the applied

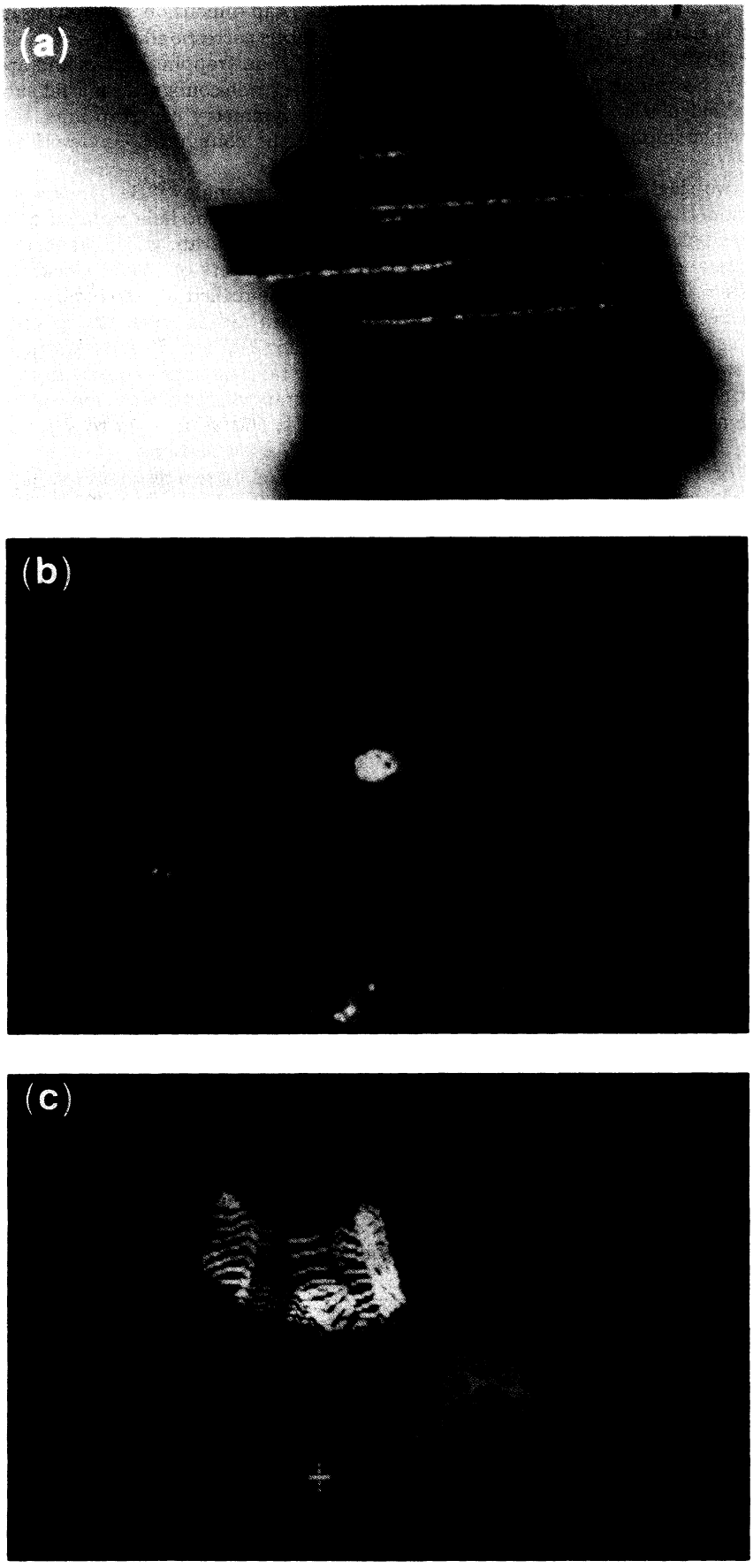

FIG. 3. (a) A three-hole trap made of Be-Cu sheets, 25 μm thick and held together with Be-Cu spacers in a macor clamp. The radius of the inner and outer holes and the spacing between sheets is $(a, \bar{a}, b) = (200, 300, 200)$ μm. (b) and (c) A single laser-cooled $^{138}Ba^{+}$ ion at the center of a three-hole trap, $(a, \bar{a}, b) = (80, 170, 100)$ μm, as observed with an imaging photomultiplier. Scattered laser light at 493.4 nm shows (c), the intensity profile in the x-y plane with a half width–half maximum of 1.0 μm, and (b) an overexposed ion image that reveals the edge of the 80-μm radius hole where the edge scattering intensity is greatly reduced by an aperture in the microscope.

potential. When the trap dimensions are in the ratio $(a{:}b{:}\bar{a}) = (1{:}0.833425{:}0.381629)$, the trap is harmonic to eighth order with $a_2 = 1.160$, $a_4 = -4 \times 10^{-6}$, $a_6 = -2 \times 10^{-5}$, $a_8 = -0.5$ [12]. As an example, assuming the above ratio with $a = 50$ μm, a numerical calculation yields the three-ring capacity $C = 21.8$ μm, which implies an efficiency $\epsilon = 0.55$.

Other simple configurations such as the two-ring and two-hole traps also can exhibit compensation that improves the harmonic content. Assuming two rings at the same potential, of the same radius a, and one above the other with spacing b, we find that when $b/a = 0.723$ or 3.39 a trap is created at the symmetry point between the rings, which is harmonically compensated to sixth order. Similarly, for the two-hole trap, assuming two sheets of radius c at the same potential with spacing b and two concentric holes of radius a, the compensation is to sixth order for $b/c = 0.25$ and $b/a = 1$.

Figure 2 compares numerical solutions of Laplace's equation of the z component of the electric field $E(z, \rho = 0) = -\frac{d\Phi(z,\rho=0)}{dz}$ for the Paul and four planar microtraps. In each case, the central electrode has a 50-μm radius and an applied peak potential of 1 V, the outer two electrodes being at 0 V. The three-ring trap (b) is the most efficient approaching the Paul trap (a) and is also superior because of its linearity up to eighth order. Of the planar traps, the three-hole trap (c) possesses the largest trapping volume and is more efficient and linear than the one-ring trap (d). The one-hole trap (e) is the least efficient when the infinite applied potential and interelectrode spacing b are replaced by finite values, making $\epsilon < 2/\pi$. The efficiency of the one- and three-ring configurations also decreases with decreasing cross-sectional radius d due to a decreasing capacity.

The above ideas can be generalized in the following way. First note that the Legendre series

$$\Phi(r, \theta) = \sum_{l=0}^{\infty} (a_l r^l + b_l / r^{l+1}) P_l(\cos\theta) \qquad (10)$$

is a general solution to Laplace's equation in spherical coordinates when cylindrical symmetry exists where the coefficients a_l and b_l depend on the boundary conditions [10]. When the potential is also symmetric to reflection along the z axis, the a_l terms are of even order in l. In addition, for an oscillating potential, the leading term $a_2 r^2 P_2(\cos\theta)$ is the quadrupole potential of a Paul trap and is responsible for stable ion trapping. Analytic and numerical solutions [13] reveal that the higher-order terms generally play a perturbative role near the origin and become significant only when the ion position approaches the characteristic trap dimension a, resulting in a less stable trap. The b_l terms correspond to the far field where ion scattering rather than trapping occurs and are of odd order. Hence, any electrode configuration that satisfies cylindrical and axial symmetry can trap ions, the Paul and linear traps and the configurations described here being examples.

Experiment. Large clouds or single $^{138}Ba^+$ ions were stored in three-hole traps with inner hole radii of $a =$ 400, 200, and 80 μm. The 80-μm trap, which we examine here, was made of Be-Cu sheets of 25-μm thickness $\times$ 1000-μm diameter, machine-drilled at its center with 80- (inner) or 170- (outer) μm radius holes, the spacing between adjacent sheets being 100 μm. In a background pressure of 10^{-10} Torr, neutral Ba atoms vaporize from a nearby oven and enter the trap where they are ionized by an electron beam (400 nA at 500 V) focused to a 2-mm diameter. Loading occurs in a few seconds.

The Ba^+ ions are laser cooled by two resonant overlapping dye laser beams (2 to 200 μW each) at 493.4- and 649.9-nm wavelength that are focused to a 40-μm beam waist at trap center with a 64° angle of incidence to the radial plane of the inner hole. Figure 3 shows the blue-light scattering image (resolution: 2 μm) of a single Ba^+ ion and the edge of the 80-μm hole as viewed through a window using a 75$\times$ microscope and imaging photomultiplier. The image elongates radially when an rf probe, applied across the electrodes, resonates the radial secular frequency, yielding, for example, $\omega_r/2\pi = 8.15$ MHz for a 352-V_{rms} rf drive at $\Omega/2\pi = 51.14$ MHz. This secular frequency corresponds to the stiffest spring constant observed in a Paul-like trap as well as an efficiency relative to a Paul trap of $\epsilon = 0.41$, where $q_r = 0.43$. At $q_z = 0.99$, a one-ion instability appears, being 10% larger than the Paul-trap instability due to the anharmonic terms, in agreement with numerical one-ion-dynamics calculations of a one-hole trap. For the case of two trapped Ba^+ ions, we calculate that the mean ion-ion distance compresses to 0.94 μm at this elevated micromotion frequency, which will now permit superradiance studies, for example. A dense Ba^+ cloud of 10-μm radius is observed in the 80-μm trap, but additional work is needed to characterize its structure.

The planar structure of these traps suggests photolithographic fabrication with the advantages of design flexibility and precision in micrometer dimensions. In addition, arrays of traps can be generated easily, and with one ion in each trap, an atomic clock superior to a one-ion clock results. Photolithographic traps are being prepared at this time.

[1] H. Dehmelt, Rev. Mod. Phys. **62**, 525 (1990).
[2] D. J. Wineland and W. M. Itano, Phys. Today **40** (6), 34 (1987).
[3] W. Paul, Rev. Mod. Phys. **62**, 531 (1990).
[4] N. Yu, *et al.*, J. Appl. Phys. **69**, 3779 (1991); H. Straubel, Naturwissenschaften **18**, 506 (1955).
[5] D. J. Wineland *et al.*, IEEE Trans. Ultrason. Ferroelec. Freq. Contr. **37**, 515 (1990); J. D. Prestage, G. R. Janik, G. J. Dick, and L. Maleki, *ibid.* **37**, 535 (1990).
[6] E. C. Beaty, J. Appl. Phys. **61**, 2118 (1987).
[7] Patent pending.
[8] J. C. Bergquist *et al.*, Phys. Rev. A **36**, 428 (1987).
[9] W. R. Smythe, *Static and Dynamic Electricity*, 3rd ed. (Hemisphere, New York, 1989), p. 171.
[10] J. D. Jackson, *Classical Electrodynamics*, 2nd ed. (Wiley, New York, 1975), pp. 90, 93, 121.
[11] L. D. Landau, E. M. Lifshitz, and L. P. Pitaevskii, *Electrodynamics of Continuous Media, Volume 8*, 2nd ed. (Pergamon, New York, 1984), p. 8.
[12] For anharmonic corrections in a Penning trap, see L. S. Brown and G. Gabrielse, Rev. Mod. Phys. **58**, 233 (1986).
[13] L. Reyna and R. G. Brewer (unpublished).

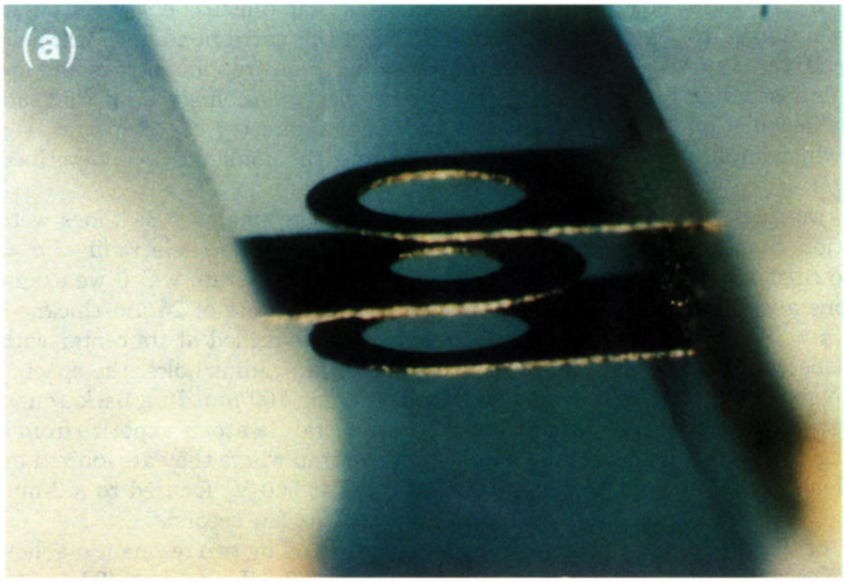

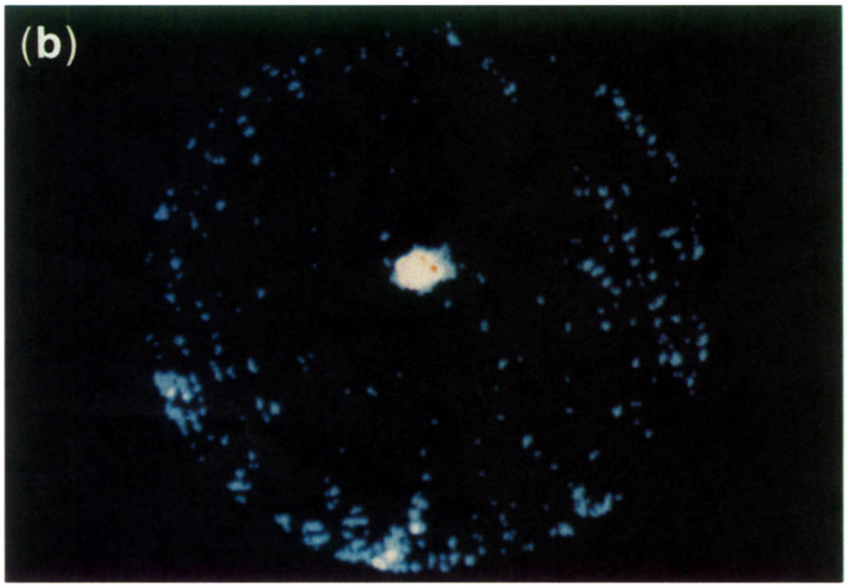

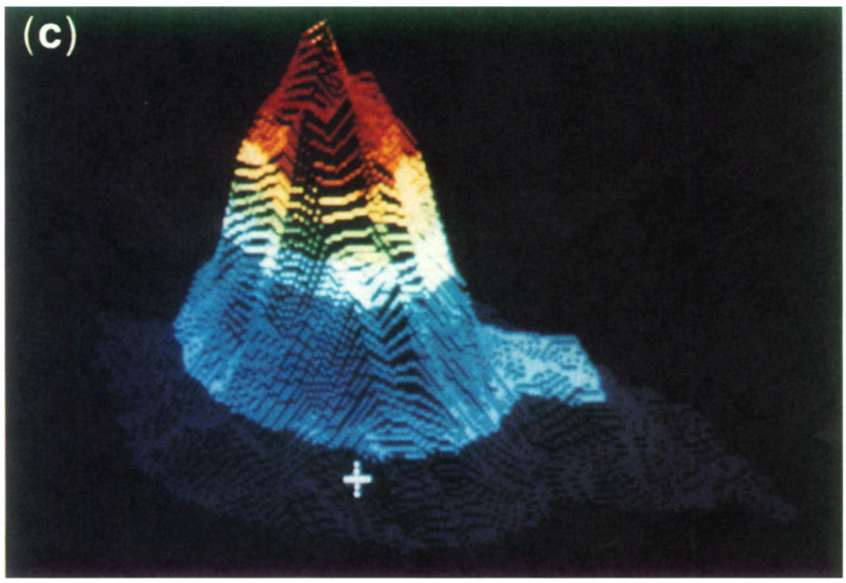

FIG. 3. (a) A three-hole trap made of Be-Cu sheets, 25 μm thick and held together with Be-Cu spacers in a macor clamp. The radius of the inner and outer holes and the spacing between sheets is $(a, \bar{a}, b) = (200, 300, 200)$ μm. (b) and (c) A single laser-cooled $^{138}Ba^{+}$ ion at the center of a three-hole trap, $(a, \bar{a}, b) = (80, 170, 100)$ μm, as observed with an imaging photomultiplier. Scattered laser light at 493.4 nm shows (c), the intensity profile in the x-y plane with a half width–half maximum of 1.0 μm, and (b) an overexposed ion image that reveals the edge of the 80-μm radius hole where the edge scattering intensity is greatly reduced by an aperture in the microscope.